

# Transmission measurements of lead fluoride ( $\text{PbF}_2$ ) crystals for the Deeply Virtual Compton Scattering (DVCS) experiment.

Sylvain Grégoire  
Graduate student in Joseph Fourier Université, Grenoble, France  
Ohio University

August 16, 2007

## Abstract

*The goal of this internship is to develop an apparatus able to measure lead fluoride ( $\text{PbF}_2$ ) blocks light transmission. Actually, this device will be used to check the behaviour on high dose of radiation of the future  $\text{PbF}_2$  electromagnetic calorimeter that will be used in the next DVCS experiment in Jefferson lab, Hall A. Therefore, measuring  $\text{PbF}_2$  light transmission is the first step to measure their transmission variation with high radiation dose. That is why this report will concentrate on relative and not absolute transmission. Moreover, this damages due to radiation might be cured by exposure to UV light.*

## 1 Introduction

The DVCS experiment at Jlab Hall A will measure the cross-section of the reaction  $\bar{e}(p, p')e'\gamma$  by scattering a high energy polarized beam off a liquid hydrogen target. The goal is to study the distribution of quarks inside the proton as a function of their spacial distribution and their momentum distribution. The radiated photon  $\gamma$  of large energy is detected in  $\text{PbF}_2$  blocks in which it makes up an electromagnetic shower: it produces a cascade of photons of smaller energies which are transmitted to the end of the blocks and transformed in electrical signal by photo-electric effect. Under harsh radiation conditions, the transmission properties of the blocks decrease to a point where the initial high energy photon cannot be detected anymore. One of the goals of the Ohio University group is to be able to restore the transmission properties of the blocks by exposing them for a few hours to UV light.

The project of this internship is to develop a bench laboratory which allows to measure the transmission of the  $\text{PbF}_2$  blocks along their length. The basic work involves interfacing a commercial photo-spectrometer with a computer, taking transmission data on a dozen of  $\text{PbF}_2$  blocks as proof of the system performance.

This internship's report will present the global and theoretic context (Section 2). Next, it will show the different tests performed (section 3) , and the  $\text{PbF}_2$  transmission results found with this apparatus (Section 4).

# Contents

<b>1</b>	<b>Introduction</b>	<b>1</b>
<b>2</b>	<b>Lead fluoride (PbF<sub>2</sub>) crystals used on Deep Virtual Compton Scattering (DVCS) project at Jlab, Hall A</b>	<b>4</b>
2.1	Generalized Parton Distribution (GPDs), Deep Virtual Compton Scattering (DVCS) . . . . .	4
2.2	Electromagnetic calorimeter . . . . .	5
2.3	Optical properties . . . . .	6
2.4	PbF <sub>2</sub> crystals properties . . . . .	7
<b>3</b>	<b>Description of blocks transmission measurements</b>	<b>8</b>
3.1	Transmission measurements . . . . .	8
3.2	Ocean Optics Apparatus . . . . .	9
3.2.1	Photospectrometer . . . . .	9
3.2.2	Deuterium-Tungsten Halogen lamp . . . . .	10
3.3	Preliminary tests . . . . .	10
3.3.1	Spectrometer calibration check . . . . .	10
3.3.2	Lamp stability . . . . .	12
3.3.3	Signal variation moving the fiber holder . . . . .	12
3.3.4	Contribution of light other than deuterium lamp . . . . .	13
<b>4</b>	<b>PbF<sub>2</sub> blocks transmission measurements</b>	<b>14</b>
4.1	Observations . . . . .	17
4.1.1	Transmission larger than 100% . . . . .	17
4.1.2	Visual comparison . . . . .	18
<b>5</b>	<b>Future</b>	<b>19</b>



## 2 Lead fluoride ( $\text{PbF}_2$ ) crystals used on Deep Virtual Compton Scattering (DVCS) project at Jlab, Hall A

After a first successful experiment on the DVCS in Jlab Hall A, the DVCS collaboration want to go further in its nucleon study using the same method kinematic settings. Most of the experimental apparatus (including the  $\text{PbF}_2$  calorimeter) will be reused for this purpose. The crystals studied during the internship were part of this previous experiment and have already been exposed to radiation harsh conditions.

### 2.1 Generalized Parton Distribution (GPDs), Deep Virtual Compton Scattering (DVCS)

The Generalized Parton Distributions (GPDs) are a theoretic concept used to describe the nucleon structure. By unifying the Feynman Parton distribution and the electromagnetic form factors, the GPDs give for example information on the distribution of quarks inside the proton simultaneously as a function of their spacial and momentum distribution (see Fig1).

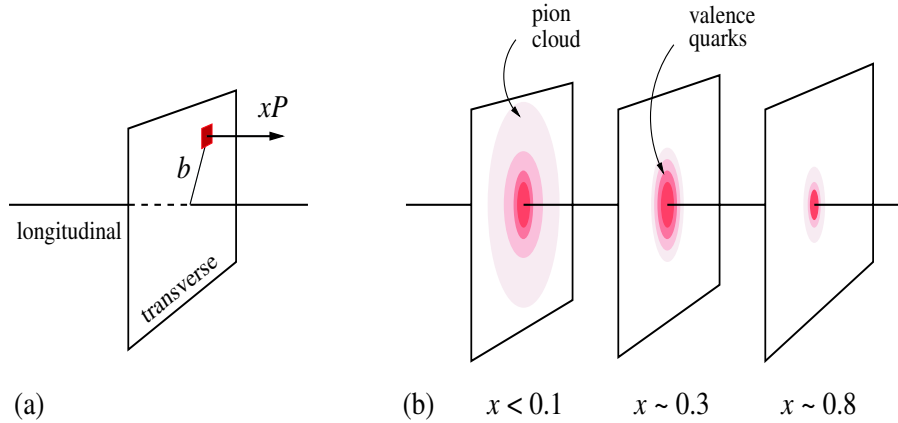


Figure 1: *Nucleon tomography : the GPDs describes the simultaneous distribution of quarks with respect to longitudinal momentum,  $xP$ , and the transverse position,  $b$ , in the infinite momentum frame. The GPDs are 3-dimensional ‘tomographic’ images of the quark structure of the nucleon, which allows one to clearly identify the different spatial distributions of the valence quarks ( $x \geq 0.3$ ,  $b \sim 1/\Lambda_{QCD}$ ) and the pion cloud ( $x \leq 0.1$ ,  $b \sim 1/M_\pi$ ) Figure from [1]*

The Deep Virtual Compton Scattering (DVCS) process is the simplest way to measure experimentally the GPDs. In this process, an electron (or a positron) collides a nucleon, and strikes a quark inside the nucleon, giving him extra energy. This quark then emits a photon  $\gamma$ , and is reabsorbed by the nucleon (see Fig 2)[2]. This process can be measured in the exclusive electro-production reaction  $ep \rightarrow ep\gamma$  in deep inelastic scattering kinematics.

The DVCS experiment at Jlab in Hall A uses a high energy polarized electron beam colliding a hydrogen target. The radiated photon is detected by a  $\text{PbF}_2$  electromagnetic calorimeter while the scattered electron is detected by the “standard” Hall A high resolution spectrometer [3]. The electromagnetic calorimeter is located between 1m and 3m from the 20cm liquid hydrogen target. with an electron beam intensity of the

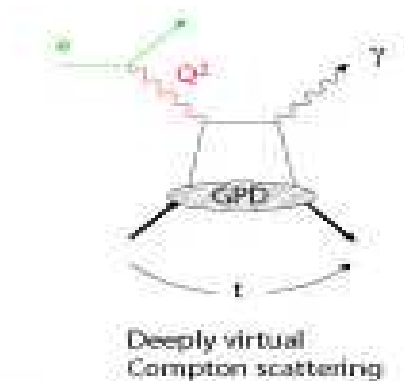


Figure 2: *DVCS with a photon emitted by a quark. The quark is then reabsorbed by the proton*

order of  $5\mu\text{A}$ .

## 2.2 Electromagnetic calorimeter

An electromagnetic calorimeter detects particles interacting with electromagnetic force. When a high energy particle is incident to an absorber, it creates a particles shower or cascade which can be detected (Fig3). The detection of the shower gives information on the incoming particle as the energy, the position where the particle arrived into the absorber,...[4].

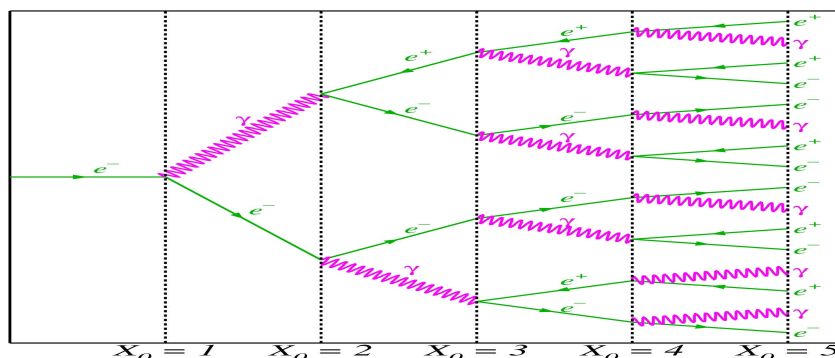


Figure 3: *Electromagnetic shower : an incident electron creates an electromagnetic shower.  $X_0$  is the medium radiation length. It corresponds to the length required to reduced the energy of charged particles by the factor  $1/e$  [4])*

In the DVCS experiment, a homogeneous non-scintillating Cherenkov radiator is used, composed by  $13 \times 16 = 208$   $\text{PbF}_2$  blocks (the electromagnetic calorimeter used for the previous experiment is shown in Fig4). Each block is measuring  $3 \times 3 \times 18.5\text{cm}^3$ , and has a PhotoMultiplier Tube (PMT) at the end. The Cherenkov photons emitted by the charged particle of the electromagnetic shower are collected by the PMTs.

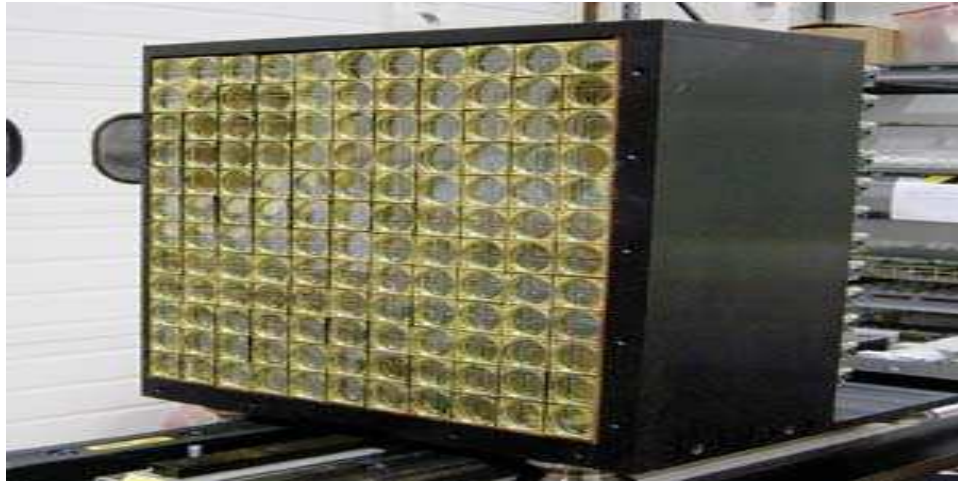


Figure 4: *The PbF<sub>2</sub> electromagnetic calorimeter used by the DVCS Collaboration in Hall A for the initial experiment*

### 2.3 Optical properties

This internship is about light transmission. So, before presenting PbF<sub>2</sub> crystals properties, it is important to talk about optical properties.

Fig5 shows the behaviour of an incident light flux going through a medium. A part of the flux  $R$  is reflected by the medium surface (reflexion). An other part  $A$  is absorbed by the medium under the form of heat, electric energy,...(absorption). The last part  $T$  is the fraction of light emerging from the sample (transmission) [5].

In all cases,

$$R + A + T = 1 \quad (1)$$

The transmission depends on reflection losses. They can be determined by the Fresnel equation

$$R = \left(\frac{n - n'}{n + n'}\right)^2 \quad (2)$$

with  $n$  and  $n'$  are indexes of first and absorber medium, assuming perpendicular incident light and a perfectly flat surface.

## Transmission, Reflection and Absorption

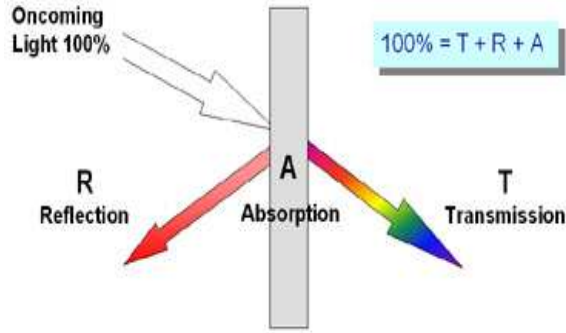


Figure 5: *Reflection, absorption and transmission*

### 2.4 $\text{PbF}_2$ crystals properties

$\text{PbF}_2$  is a pure Cherenkov radiator. With a density for  $\rho$  of  $7.77\text{g/cm}^3$ , a radiation length  $X_0$  of  $0.93\text{cm}$  and a Molière radius  $R_M$  of  $2.2\text{cm}$ , this material allows a compact detector [6]. Each DVCS block is around 19 radiation lengths, so 99.9% of the energy from the incoming particle is absorbed. Moreover,  $\text{PbF}_2$  presents a good radiation resistance, which allows to put the detector close to the target. But  $\text{PbF}_2$  light transmission still decreases with high radiation dose. P. Achenbach (Mainz, Germany)[7] measured the  $\text{PbF}_2$  transmission decrease between 200nm and 800nm for different doses as shown in Fig6. Most of the effect is in the blue and UV range, which happens to be the Cherenkov light and the DVCS PMT sensitivity wavelength range.

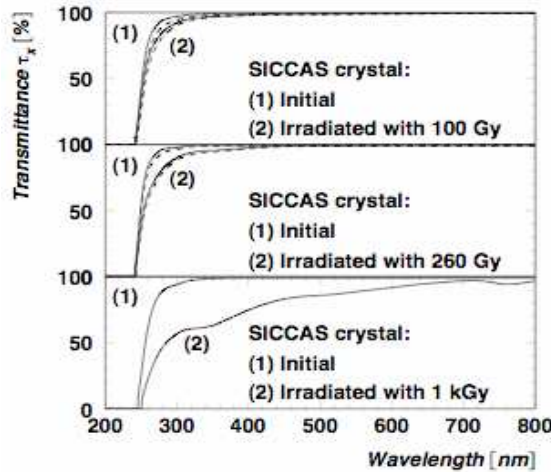


Figure 6: *P. Achenbach's results with high dose of radiation on  $\text{PbF}_2$  blocks (SICCAS is the blocks manufacturer)*

Under dose accumulated, the blocks transmission can decrease to a point where only a few photons per incoming high energy photon will reach the PMT, such that the signal will be lost. P. Achenbach also found that it was possible to cure this transmission decrease, by exposing the damaged blocks to UV light. The future DVCS experiments will deposit a dose around seven times higher than the maximum used by P.

Achenbach (around 7kGy). The plan of the DVCS collaboration is to cure the blocks seven times during the data taking. Therefore, the collaboration plans to repeat P. Achenbach's tests to learn the how to of this method as well as the effect of repeated curings. A device capable of measuring transmission through the block is therefore needed and its development is the goal of this internship.

Moreover, transmission also depends on quality of the block. Actually, impurities in a block or on its surface can decrease its transmission[8]. So, to detect them, transmission measurements must be done transversely, for different positions along the length of the blocks.

### 3 Description of blocks transmission measurements

#### 3.1 Transmission measurements

The goal is to measure PbF<sub>2</sub> crystals light transmission between 200nm and 800nm with a precision of maximum 5%, because transmission decrease is known to be in this wavelength range and to be of the order of 20% for a dose of 1kGy.

Transmission was measured for several blocks, along their width (Fig7), in different points of each block (10 measures per block). Moreover, measurement were done following equation 3:

$$T(\lambda) = \frac{S(\lambda) - B}{L(\lambda) - B} \quad (3)$$

where  $\lambda$  is the wavelength, T is the transmission, S is the spectrum of the light going out of the block, L is the signal of the lamp spectrum without the block, and B is the background.

The background is electronic; because of the nature of the spectrometer, there is always a residual signal that must be taken into account in the other signals. So, for example, the true  $S(\lambda)$  is the one that is measured minus the residual background.

The equation 3 gives the measured coefficient of transmission, but the quantity of interest is the absorption A. Indeed, the surface quality is not changed by radiation exposure but absorption is. Moreover one should note that in the actual DVCS experiment, the high energy photon penetrates inside the block before starting to develop an electromagnetic shower. Also the PMT is optically coupled to the PbF<sub>2</sub> block. Therefore, R is irrelevant for the actual DVCS experiment even though it is actually measured by the device developed in this project. Using equation1, absorption is:

$$A = 1 - T - R \quad (4)$$

Reflexion must also be taken into account. Therefore, light is lost twice by reflexion, because of the two surfaces of the PbF<sub>2</sub> blocks. Using the Fresnel equation seen in section 2.3, and assuming a normal incident light with two perfectly flat parallel surfaces, the coefficient of reflexion is:



$$R = \frac{(4n')^2}{(1 + n')^4} \quad (5)$$

with  $n'$  the  $\text{PbF}_2$  index ( $n'=1.82$ ). So, reflexion losses are for  $\text{PbF}_2$  blocks around 17%.

Transmission measured can also vary because of the fact that a block has some impurities [8].

## 3.2 Ocean Optics Apparatus

The device used for these experiments is composed of a continuous Deuterium-Tungsten halogen lamp, and a photospectrometer from Ocean Optics. Both were linked by optic fibers to a fiber holder. Blocks can be placed between the two fibers. The set up is shown in Fig7.

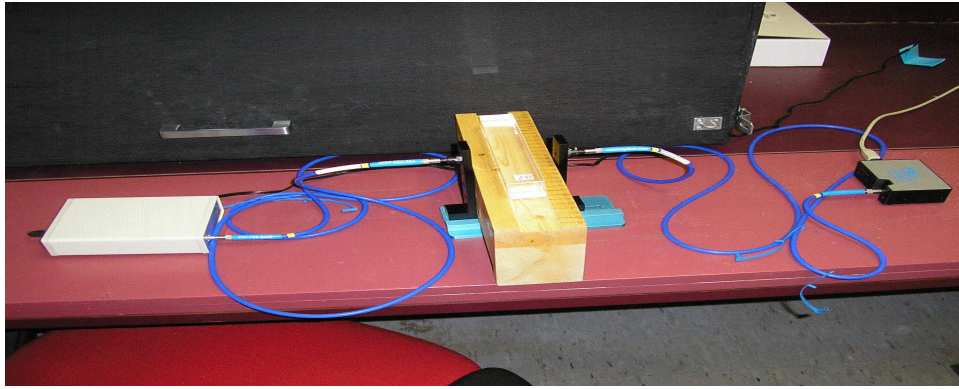


Figure 7: *Devices used : the Deuterium-Tungsten lamp on the left, the photospectrometer on the right, the fibers (blue) and the fiber holder. The wooden block (yellow) supports the blocks.*

### 3.2.1 Photospectrometer

The Ocean Optics' USB4000 photospectrometer (see Fig8) used in this project is composed of mirrors, a prism and a CCD camera. Mirrors bring light into the prism. Then, light is diffused and brought to the CCD camera. It can detect the signal as a function of the wavelength Fig8. Its sensitivity is between 200 and 1100 nm, with 3648 pixels. It has an electronic shutter for spectrometer integration times as fast as 3.8 milliseconds – a handy feature to prevent detector saturation. In addition, the USB4000 has signal-to-noise of 300:1 and optical resolution (FWHM) ranging from 0.03-8.4 nm (depending on the grating and entrance aperture selection)[9]. The spectrometer is connected to a computer via a USB port and signals are read by the SpectraSuite software [10].



Figure 8: *Inside view of the Ocean Optics USB 4000 Spectrometer. 1: connector used to plug the fiber. 2: slit acting like the entrance aperture. 3: absorbance filter, used to block second- and third- order effects or to balance color. 4: collimating mirror. 5: prism. 6: focusing mirror. 7: detector collection lens used to increase light-collection efficiency. 8: filter. 9: quartz window to enhance the performance of the spectrometer. 10: CCD camera*

### 3.2.2 Deuterium-Tungsten Halogen lamp

The lamp used for this project is the continuous DTmini Ocean Optics lamp. This is a Deuterium-Tungsten lamp. Its spectrum is shown in Fig9 and its characteristics are available in [13].

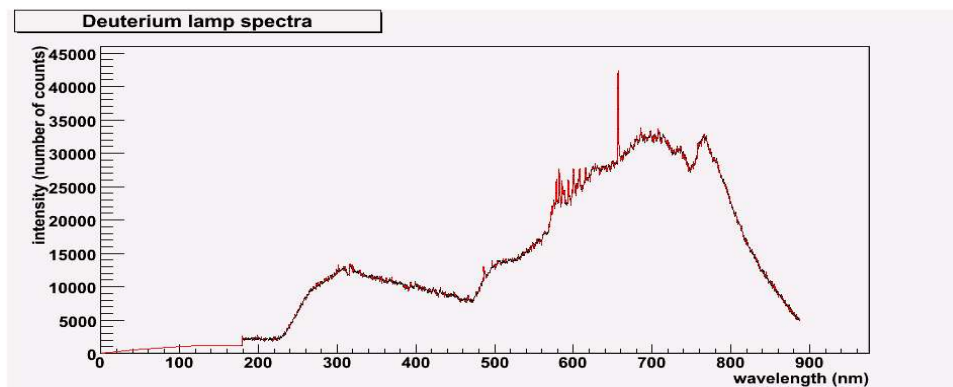


Figure 9: *Ocean Optics DTmini lamp spectrum. The shape of this spectrum represents the lamp spectrum modulated by the CCD camera sensitivity. In this project, the CCD camera detects between 200 and 900 nm. Usually, the DTmini lamp spectrum does not decrease at 200 nm and 900 nm [13]*

## 3.3 Preliminary tests

### 3.3.1 Spectrometer calibration check

After being produced, each spectrometer is calibrated in wavelength by Ocean Optics. But, in order to check this calibration, it was decided to make some calibration measurements. Four fluorescent lamps and a laser spectra with known rays were used; Mercury(Hg), Krypton(Kr), Hydrogen(H) and Neon(Ne) for the lamps,

and di-Nitrogen( $N_2$ ) for the laser. Fig10 shows the comparison between known rays for each light source and the test measurements. The comparison was only carried on for the main rays of each material. The difference between the known and measured rays never exceeds 1 nm. The radiation damage observed by P. Achenbach (see Fig6) are smooth such that the 1 nm deviation is more than satisfactory for the transmission discussed in this report.

The relative intensity of each ray for one lamp cannot be used to measure the detection efficiency of the CCD camera. Indeed those ratios depend on temperature and pressure [12]. Because the ultimate goal of this project is to measure transmission, a ratio where the CCD detection efficiency cancels, the detection efficiency calibration was not pursued.

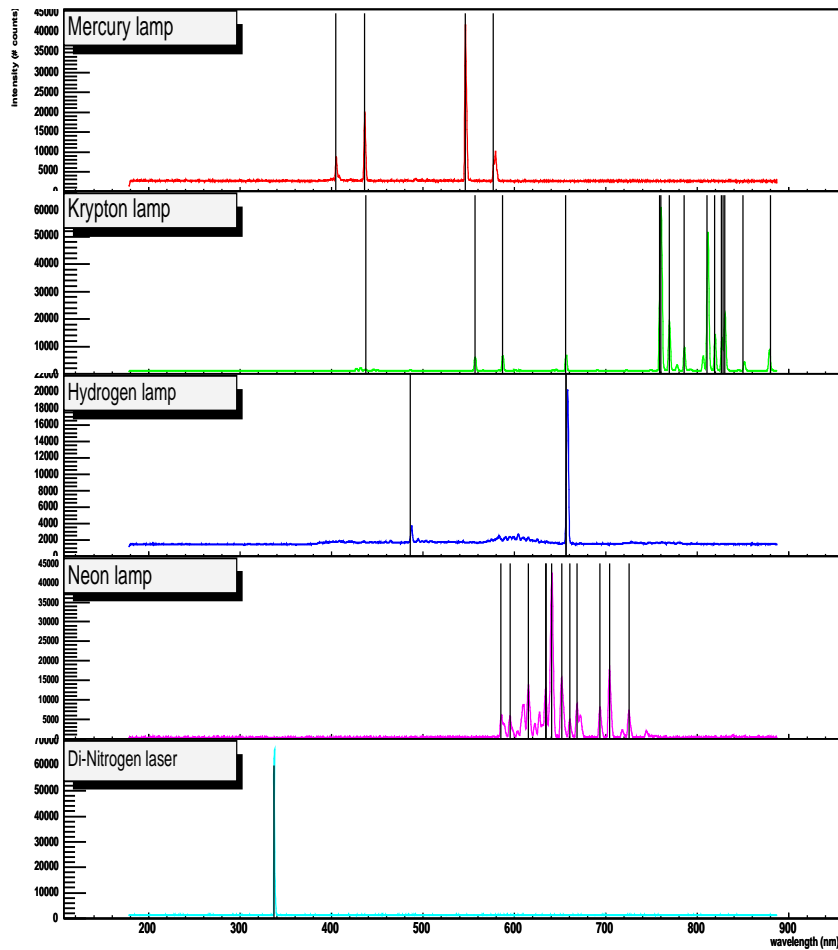


Figure 10: *This figure represents intensity in number of counts as a function of the wavelength in nm. The measured spectrum for each light source are in color. Black lines represent expected lines from [11]*

Hydrogen measured spectrum presents an unexpected fluctuation around 600 nm. This fluctuation disappears with a 300-700 nm band pass filter. Being around 600nm, this fluctuation is due to a higher order of an other ray in the spectrum. Moreover, the Neon and Krypton spectra in Fig10 show unexpected rays. Indeed, only the main rays of the expected spectrum were used for the comparison measured-expected rays. The rays represent other little rays.

### 3.3.2 Lamp stability

The plans for measuring the transmission through the blocks is to successively measure the spectra  $S$  for 10 positions along the block and to use measurements of the lamp spectrum  $L$  done before and after the measurements of  $S$ . This method relies on the device being stable during the measurements of  $S$ , because it can be around 10 minutes long. Fig11 and Fig12 shows that the device is stable at better than 0.5% after the first hour. So, transmission measurements must be done after leaving all the apparatus working for a certain amount of time

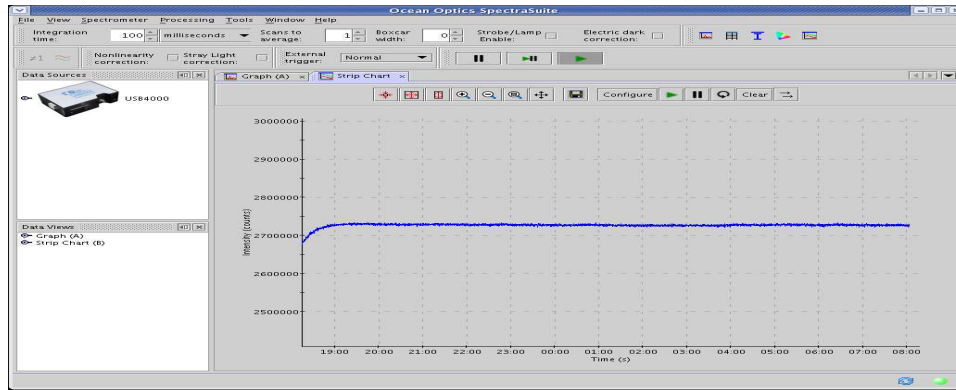


Figure 11: This figure shows the integration between 200nm and 800nm of the background spectrum as a function of time. This screen capture shows the Ocean Optics SpectraSuite software used in this project.

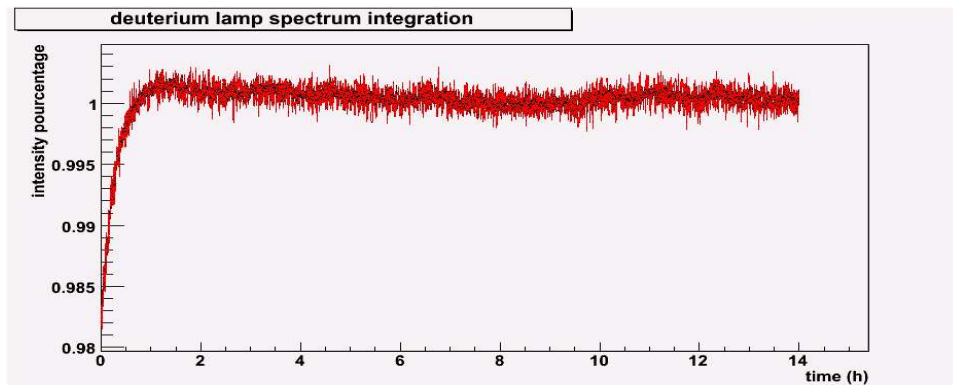


Figure 12: This figure shows the integration between 200nm and 800nm of the lamp spectrum as a function of time. Intensities for every point of the graph were divided by the last point intensity.

### 3.3.3 Signal variation moving the fiber holder

Moreover, following the previous part, the original plans were to move the fiber holder while the blocks stay put to make measurements of  $S$ . The manipulation of the fiber holder revealed that the straight through spectra  $L$  were unstable. Fig13 shows that the signal can vary by up to 10% if between each measurement the fiber holder is shaken. As a conclusion, the fiber holder must not be moved, and the blocks would move instead.

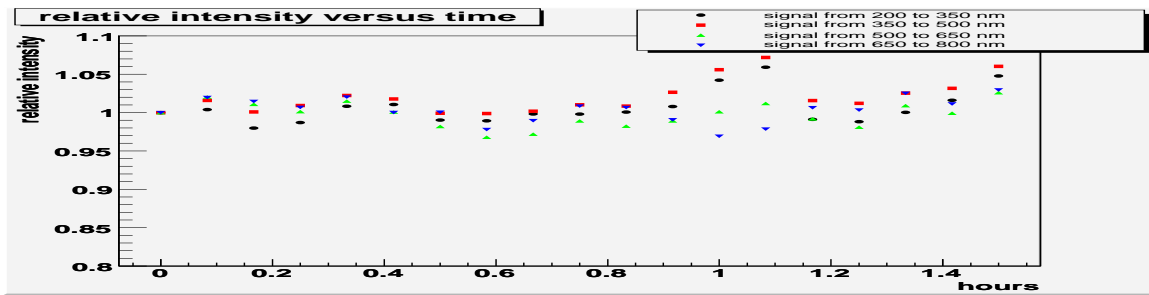


Figure 13: During 1.5 hours, shakings of the fiber holder were done every 5 minutes. Measurements of the signal were done right after. This graph shows the integration of the signals as a function of time for different wavelength ranges. Actually, each integration was divided by the first one.

### 3.3.4 Contribution of light other than deuterium lamp

The measure of transmission presented in equation 3 assumes that the background level  $B$  is the same for the straight through measurement  $L$  and the signal emerging from the block  $S$ . The background level has two components.  $E$  the electronic noise and  $O$  the background level due to ambient light such that Fig 14 shows the evaluation of  $E$  and  $O$  in the lab space of the internship.  $B$  is measured with the DTmini lamp off but the ambient lamp on.  $E$  is measured with a cap covering the entrance part of the photospectrometer (position 1 in Fig 8). These measurements show that for this lab space,  $O$  represents 0.5% of the signal  $L$  or  $S$ . In the conditions of this lab space, one can conclude that the variation of  $O$  between the measurement of  $L$  and  $S$  will lead to a neglectable (less than 5%) bias on the evaluation of the transmission. Moreover one needs to keep in mind that ultimately the effect studied for the DVCS is the variation of transmission before and after curing. In the limit where the ambient light does not vary during the curing period, its bias effect on  $T$  is irrelevant.

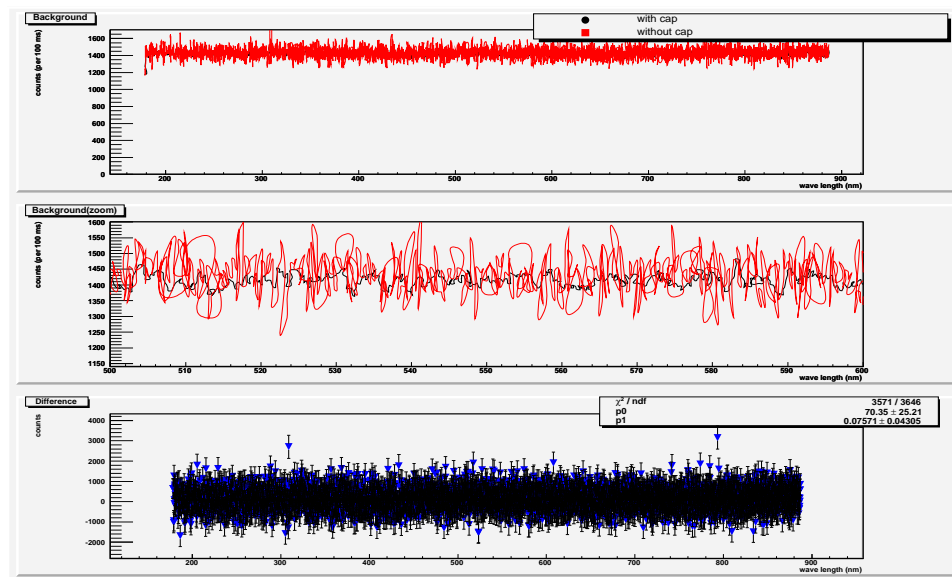


Figure 14: This figure shows the two background measurements in the upper part and the difference between both in the lower part. The spectrum without cap is a measurement of  $B=E+O$  while the spectrum with the cap is a measurement of  $E$ . A fit of this difference was done. The middle part is a zoom of the upper part.

## 4 PbF<sub>2</sub> blocks transmission measurements

Transmission light measurements were done for 6 different blocks ; block 33, 39, 69, 87, 101, 120, seen in Fig15. These blocks are half of the set in storage at Ohio University. The blocks stored at Ohio University are representative of different situations along the calorimeter.

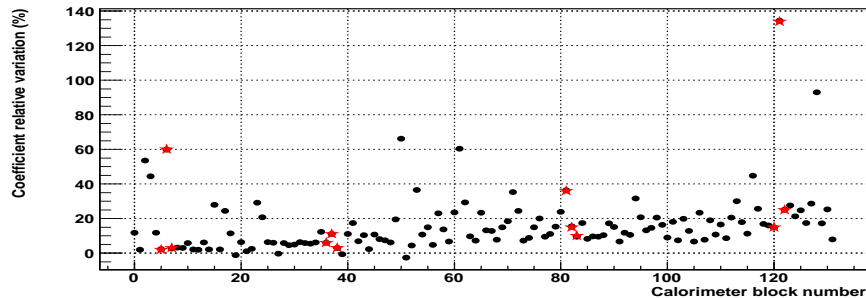


Figure 15: *This graph shows the relative variation of the calorimeter energy calibration constants between the beginning and the end of the first DVCS experiment [3]. In this figure the blocks are indexed by their trigger number. The ones with a lower trigger were away from the target. The blocks stored at Ohio University are shown in red stars. The transmissions measured so far were done on blocks 33, 39, 69, 87, 101, 120. This corresponds respectively to triggers 7, 121, 82, 81, 6, 5 in this graph.*

Fig16 to 21 show results from the transmission measurements of these six blocks. For each figure, the upper panel shows the raw data: the straight through spectra lamp measurements (L) before and after measurements along the blocks, the background measurement (B≡E) and the ten measurements of transmitted light (S) at 10 different transverse positions along the block. The lower part shows the transmission computed according equation 3 as a function of the wavelength and of the position along the block. The color scale is shown on the right. Position is taken from left to right, with the sticker showing the block number placed up-right (see Fig22). Usually, the sticker is placed on the PMTs side. The transmission decrease should be on the target side, because the energy deposited by particles is higher there. Therefore, final transmission measurements show that blocks 101 and 87 have been reversed.

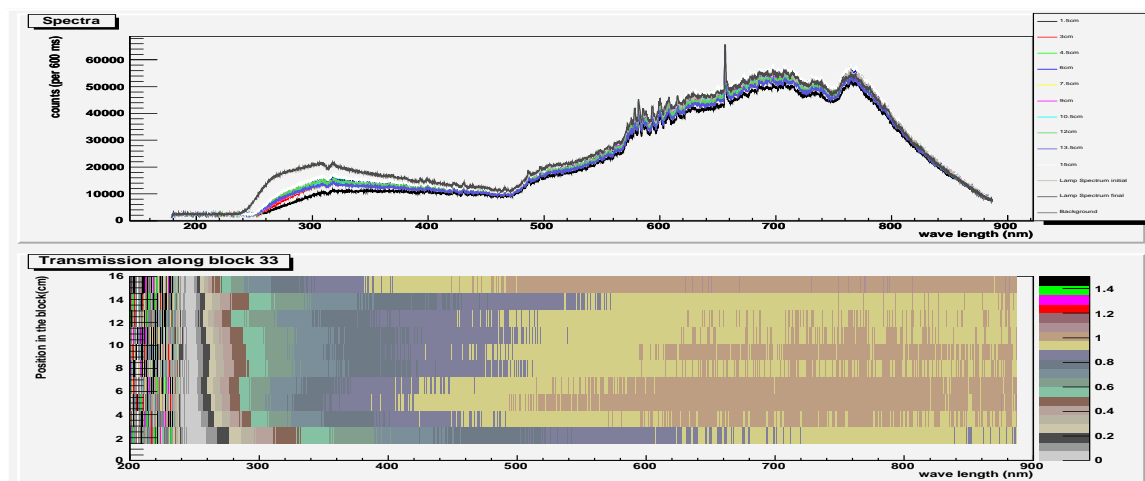


Figure 16: *Transmission measurement for block 33.*

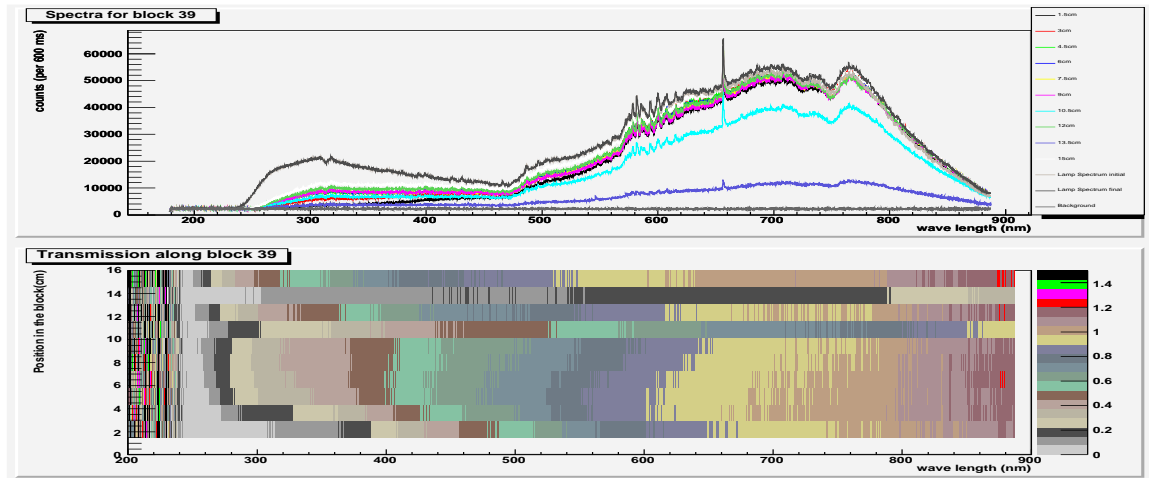


Figure 17: *Transmission measurement for block 39.*

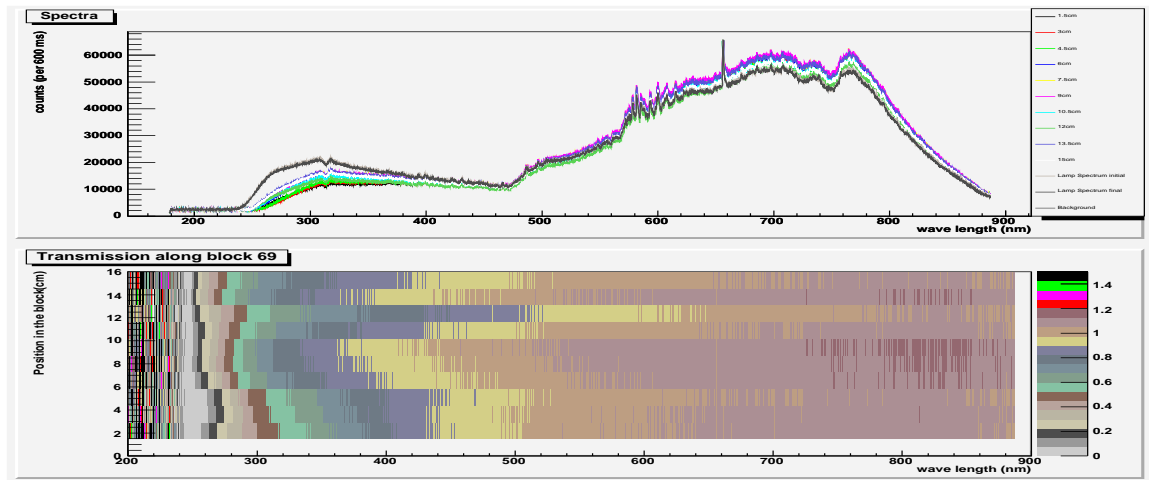


Figure 18: *Transmission measurement for block 69.*

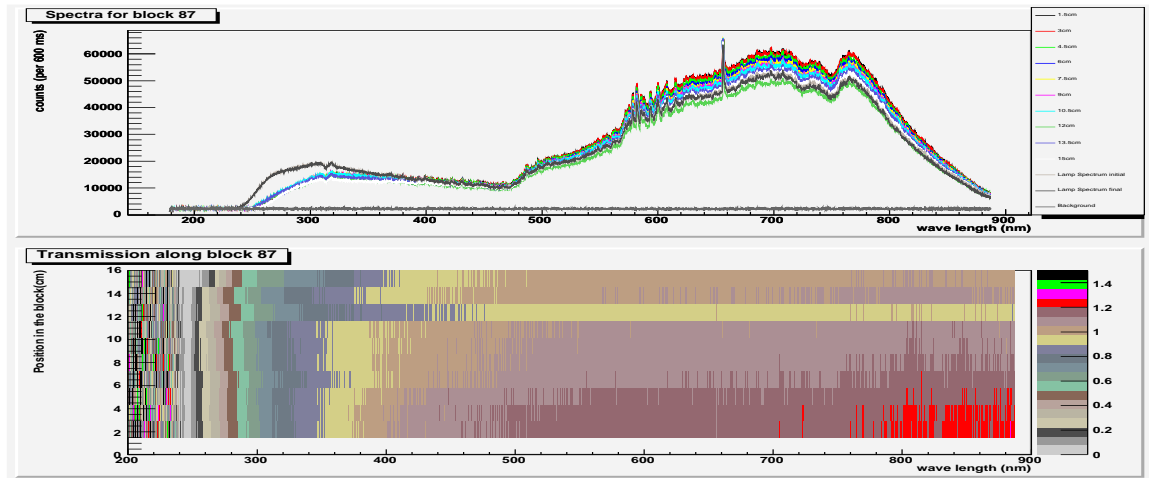


Figure 19: *Transmission measurement for block 87.*

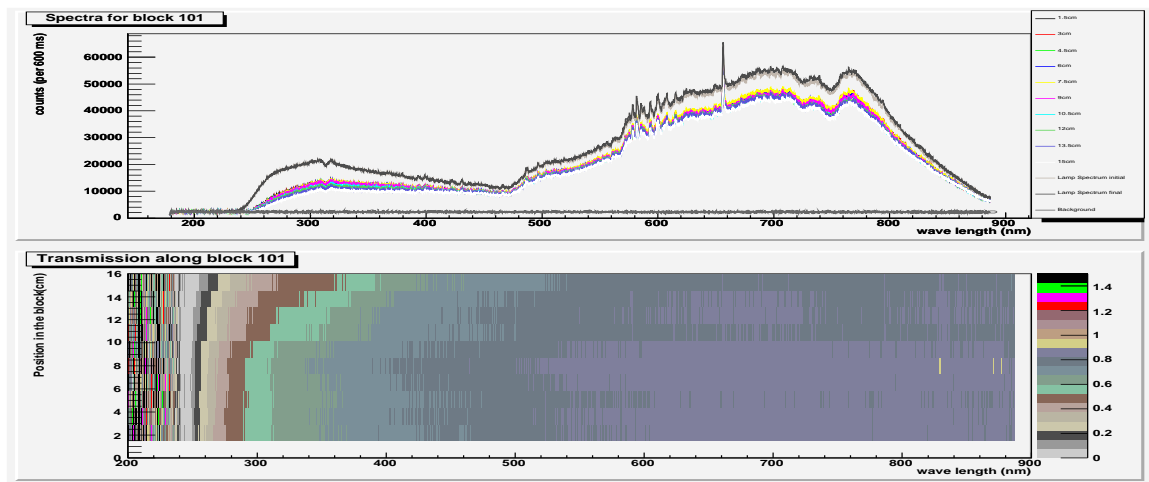


Figure 20: *Transmission measurement for block 101.*



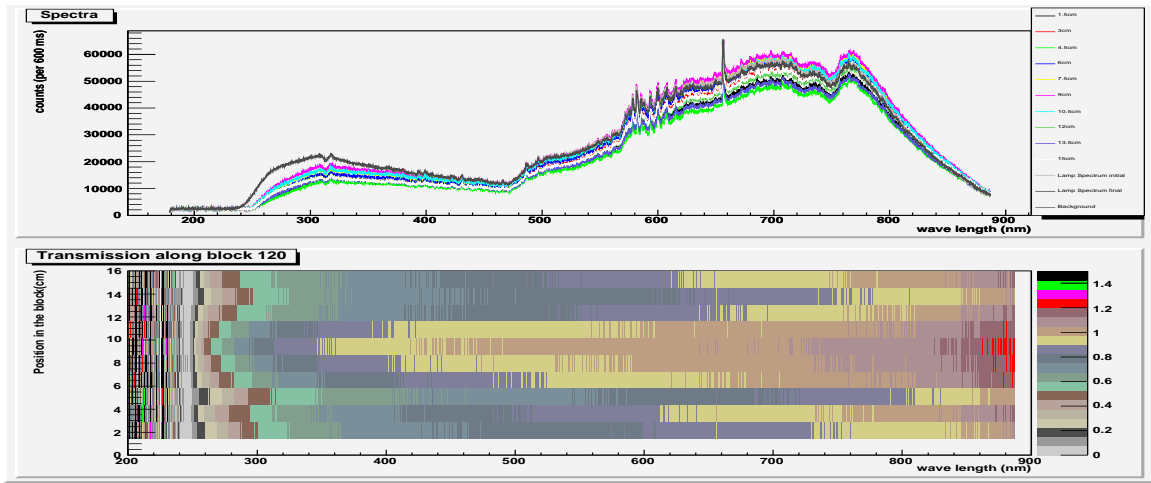


Figure 21: *Transmission measurement for block 120.*

## 4.1 Observations

### 4.1.1 Transmission larger than 100%

Blocks present a transmission that can be higher than 100%. Because the ultimate DVCS goal is a relative transmission, this anomaly is not really important. Nevertheless, some tests were done to understand source of this effect.

First, the effect could be due to the outside light contribution (O) being larger when a block is in between the fiber holder harms than when the block is not in place. The measurements described in section 3.3.4 were repeated with a block. The outside light contribution was found to be less than 0.5% of L, which cannot explain a transmission of sometimes more than 120%.

Secondly the effect where the light is focused by the block was investigated. The incoming light is approximated to be only one ray. Actually, it is a cone of light. This cone gives a circle on the second fiber perpendicular plan. Using Snell's laws [14] twice for light incident into a medium with an index higher than the first medium, the radius of the circle is higher without than with the block. Assuming a medium transmission of 100%, all the photons incident go through it. So, with the same number of photons and a circle radius lower, the density of photons is higher with than without the block. For the fiber entrance surface, which does not vary, the signal is therefore higher with the block.

Finally, the large transmission could be the result of a wavelength shifting mechanism by the blocks or the detection of higher order dispersion spectrum by the CCD.

Both the focusing and the shifting hypothesis are under further investigations.

### 4.1.2 Visual comparison

Firstly, those  $\text{PbF}_2$  blocks transmission measurements help to detect impurities. Fig22 shows a visual inspection of blocks 39, 87 and 101. Everything observed on those three blocks can also be observed on the three other blocks. Making a comparison between visual inspection and transmission measurements allows to check the apparatus efficiency.

The block 39 surface is scratched. This defect is visible in the block 39 transmission measurement, for the position of 10 cm where the transmission decreased by around 20%, and for the position of 13 cm where it is decreased by more than 70% (see Fig17). This defect is found also on block 33 (see Fig16) for the position of 13 cm, and at the beginning and at the end of the block 120 (see Fig21), where the surface is also scratched. Therefore, this defect make the blocks surface not completely flat; the light reflected by the surface is then higher, decreasing the absorption  $A$ .



Figure 22: *Visual inspection of blocks 39, 87 and 101. The block 16 in this picture is actually the block 101. the surface of block 39 us scratched, and the the PMT side of blocks 39 and 101 are darkened.*

Moreover, the measured  $\text{PbF}_2$  blocks have been exposed to radiation during the first DVCS experiment. In plus of decrease in the transmission created by the scratches, they all present a transmission lower on the target side than on the PMT side. Fig22 shows that the blocks are indeed on the target side (very evident for block 39). This darkening is most likely created by electrons and photons of very little energy that do not create an electromagnetic shower. For an electromagnetic shower, the maximum energy is deposited between  $5-10X_0$ (radiation length) within the block [15]. For the future DVCS experiment, this corresponds to the half of the block. Therefore, this darkening will not interfere in the future DVCS experiment. The particles creating a shower will still deposit their energy in the middle of the block without being disturbed by the darkening.

## 5 Future

This internship is over. But there are still many tests that have to be done.

The first of them is to find a mechanism to move the blocks easily. That would allow to make automatic measurements. A moving table is now planed in Ohio University.

Secondly, section 4.1.1 showed that some hypothesis to explain the fact that  $\text{PbF}_2$  blocks transmission could be higher than 100% are still under investigation. For the focusing hypothesis, a way could be to change the length between the two fibers and to check the variation of light intensity as a function of the radius of the circle. For the shifting hypothesis, the method used in section 3.3.1 to hide Hydrogen spectrum fluctuation is planed. Simply, the goal is to use a band pass filter to know if the extra light could be a second order one.

Finally, the all apparatus will be brought to the Jefferson lab where high radiation effects will be studied. The blocs will be irradiated to doses comparable to the ones generated during the main experiment and the UV curing method tested.

## 6 Conclusion

During this internship, an apparatus able to measure the lead fluoride ( $\text{PbF}_2$ ) blocks transmission was developed for the  $\text{PbF}_2$  electromagnetic calorimeter for the DVCS experiment in Jlab, Hall A. This was a part of project planning to measure the  $\text{PbF}_2$  blocks transmission variation with high radiation dose.

Different tests were done on the devices used in order to check their efficiency; the photospectrometer wavelength calibration check, the stability on time of the all system, the best experimental conditions, ...

Finally, transmission measurements were done for six of the blocks from the previous DVCS experiment in Hall A. Globally, they were all damaged by the dose they were exposed to in this previous experiment. Except for scratches on the surface of some of them, this damages will not avoid the radiated photons from DVCS to be detected as an electromagnetic shower.

The DVCS collaboration will soon be able to use the all apparatus to study high radiation effects on the  $\text{PbF}_2$  blocks transmission.

## References

- [1] *Conceptual Design Report (CDR) for the Science and Experimental Equipment for The 12 GeV Upgrade of CEBAF*, an internal report of Jlab, available at [http : //www.jlab.org/div\\_dept/physics\\_division/GeV/doe\\_review/CDR\\_for\\_Science\\_Review.pdf](http://www.jlab.org/div_dept/physics_division/GeV/doe_review/CDR_for_Science_Review.pdf)
- [2] DVCS Collaboration, (2000), Proposal to Jefferson Lab PAC 18, Deeply Virtual Compton Scattering At 6 GeV available at [http : //www.jlab.org/exp\\_prog/proposals/00/PR00-110.pdf](http://www.jlab.org/exp_prog/proposals/00/PR00-110.pdf)
- [3] C. Muñoz Camacho et al.(Jefferson lab Hall A) *Phys. Rev. Lett.*, *97:262002, 2006*
- [4] G. Gratta, H. Newman and R. Y. Zhu,(1994), “Crystal Calorimeters in Particle Physics”,*Annu. Rev. Nucl. Part. Sci.* *14:453-500*
- [5] Hans Breuer, *Atlas de la physique, p.146-147* Encyclopédies d’Aujourd’hui
- [6] D. F. Anderson, M. Kobayashi, C. L. Woody and Y. Yoshimura. “Lead Fluoride: an ultra-compact Cherenkov radiator for em calorimetry”, *Nucl. Instrum. Meth. Phys. Res., vol.A290, pp. 385-389, May 1990*
- [7] P. Achenbach et al., “Radiation resistance and optical properties of lead fluoride Cherenkov crystals”,*Nucl. Instrum. Meth. Phys. Res., vol. A416 357-363,1998*
- [8] P. Achenbach , “Observation of Scattering and Absorption Centers in Lead Fluoride Crystals” *arXiv:nucl-ex/0606027 v1 22 Jun 2006*
- [9] [http : //www.oceanoptics.com/products/usb4000.asp](http://www.oceanoptics.com/products/usb4000.asp)
- [10] [http : //www.oceanoptics.com/products/spectrasuite.asp](http://www.oceanoptics.com/products/spectrasuite.asp)
- [11] [http : //physics.nist.gov/PhysRefData/Handbook/periodictable.ht](http://physics.nist.gov/PhysRefData/Handbook/periodictable.ht)
- [12] N. Bibinov, H. Halfmann, P. Awakowicz and K. Wiesemann “ Relative and absolute calibrations of a modern broadband echelle spectrometer” *Meas. Sci. Technol.*, *18(2007) 1327-1337*
- [13] [http : //www.oceanoptics.com/Products/dtmini.asp](http://www.oceanoptics.com/Products/dtmini.asp)
- [14] [http : //en.wikipedia.org/wiki/Snell'sLaw](http://en.wikipedia.org/wiki/Snell'sLaw)
- [15] W. M. Yao *et al.* [Particle Data Group], “Review of particle physics,” *J. Phys. G* **33**, 1 (2006).